Effect on Mass Eccentricity of Superstructure on Seismic Performance of Rocking Pillar Base Isolation System

Tomomi Fujita
Assistant Professor, Dept. of Architectural Design, Sendai National College of Technology , Sendai, JAPAN

Naoki Funaki
Associate Professor, Dept. of Architecture, Tohoku Institute of Technology, Sendai, JAPAN

SUMMARY

In developing countries in seismic areas, many people live in traditional masonry houses. Although collapse of the houses during an earthquake may result in tragic losses of human lives, a shift toward a structure based on modern engineering is difficult by socioeconomic reason. The authors have been developing new form of base isolation system for masonry houses. The system consists of rocking pillars and dampers. The rocking pillar, key component of the system, is equipped with spherical caps at top and bottom ends of the pillar. This paper presents the results of a two-directional shaking table test of a reduced scale test specimen. Based on the obtained test results, fundamental characteristics of seismic behavior and effectiveness of the system are discussed. Furthermore, to verify the validity of the developed numerical simulation program, the result of two-directional shaking table test are compared with those of the corresponding simulation by the program.

Keywords: Base Isolation, Rocking Pillar, Lead Damper, Masonry House, Shaking Table Test

1. INTRODUCTION

In developing countries in seismic area, many people have to live in traditional masonry houses of earth made material. Investigation showed that approximately 50% of the population in developing countries live in the traditional earth made construction [EERI/IAEE, 2003]. In addition, the traditional masonry houses responds very poorly to earthquake. The earthquake of M6.5, which took place in Iran on December 26 2003, totally destroyed the historical city of Bam killing about forty thousand people. More recently, many casualties due to collapsing masonry houses in developing countries during large earthquakes are reported. However, it is not easy to shift the construction of these houses to the one of the modern technology but dependence on local products of masonry material can not be changed.

In this study, as a possible solution of avoiding collapse of masonry houses, we think implementing base isolation devices to reduce input seismic force. To popularize the base isolation system widely in developing countries, the system needs to be simple to manufacture, low cost and to be installed on site by non-skilled local labors.

Taking above requirements into account, the authors have been developing a new form base isolation system for masonry houses utilized rocking pillar. In the previous paper, seismic performance of the system was discussed by one-directional vibration test of reduced scale specimen and numerical analysis [Funaki et al., 2008]. The purpose of this paper is to investigate experimentally the fundamental property of vibration response and seismic performance of the system based on results of two-directional shaking table test using reduced scale test specimen and Numerical response analysis by the use of developed program.

2. OUTLINE OF ROCKING PILLAR BASE ISOLATION SYSTEM

Figure 1 shows a masonry house provided with the proposed base isolation system. The base isolation foundation consists of rocking pillars, dampers and caissons. The rocking pillar is formed by a steel tube provided with spherical caps at the both ends.
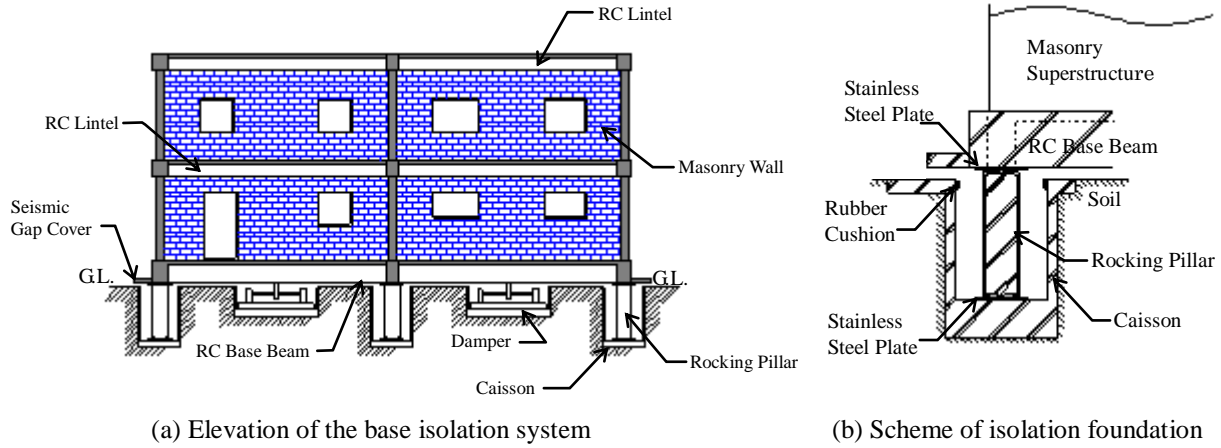
(a) Elevation of the base isolation system
(b) Scheme of isolation foundation
Figure 1. Conceptual diagram of masonry house with rocking pillar base isolation system

Figure 2 shows geometry of the rocking pillar. By making radius of curvature of the spherical cap, R, larger than half length of the pillar, L, a returning moment occurs against rocking motion rotating around the bottom end of the pillar. Consequently, superstructure supported by the rocking pillars is subjected to slow lateral vibration of long period. The natural period of the system is derived from equilibrium of moment of inertia acting on the pillar and returning moment of the pillar, as follows:

$$T = 2\pi\sqrt{\frac{2L^2}{(R-L)g}} \qquad (2.1)$$
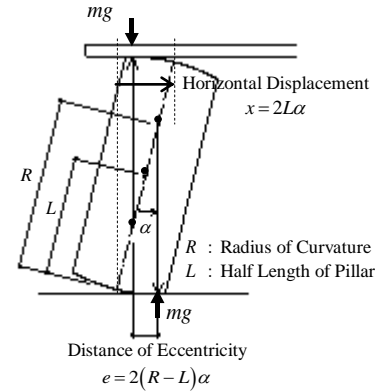
Figure 2. Geometry of Rocking Pillar

In comparison with the other isolation systems, as shown in equation (2.1), natural period of the rocking pillar base isolation foundation does not depend on mass of superstructure but is determined by dimension of the pillar, R and L. This property is attributed to returning moment of the pillar and is proportional to its vertical load. Accordingly, the presented rocking pillar base isolation system is in principle free from torsional vibration because the center of distributed returning moment automatically coincides with the center of gravity of the superstructure.

3. VIBRATION RESPONSE CHARACTERISTICS OF THE BASE ISOLATION SYSTEM

3.1. Test Apparatus Description and Test Setup

Shaking table tests were carried out on a reduced scale test specimen. Figure 3 shows detail of the test specimen and whole view of the apparatus on shaking table. The superstructure was composed of basement steel beams and weight of steel plates mounted on the basement. It was supported by four rocking pillars. Total mass of the basement including the steel plates is 1.4ton. To form the weight, steel plates were piled on the basement beams in X1 and X2 axes. The weights were arranged in two different setting: symmetric and eccentric. In the symmetric setting, two weights having same mass of 0.55ton were placed. In the eccentric type, two weight of different mass were put on each basement beam. Test case is listed in Table 1. The rocking pillar is formed by steel rods equipped with spherical

bearings of R=20cm at the both ends. The length of the pillars is 2L=34cm. The pillar was set a smooth stainless plate of 6mm. The same plate was installed between the top of the pillar and the basement beam. To avoid overturning the rocking pillar caused by excessive input, caissons made of transparent acrylic tube were set up around the pillar. As shown in Figure 3-4, dampers were installed between the basement beams and the shaking table. The damper was made from flat lead plate shaped into a circular arc (Figure 5). Harmonic excitation test have been previously conducted for this dampers, and their basic characteristics have been made clear. Based on the obtained test results, it was confirmed that the damper took the forms of stable-spindle shaped hysteresis and has a high energy dissipation capacity.
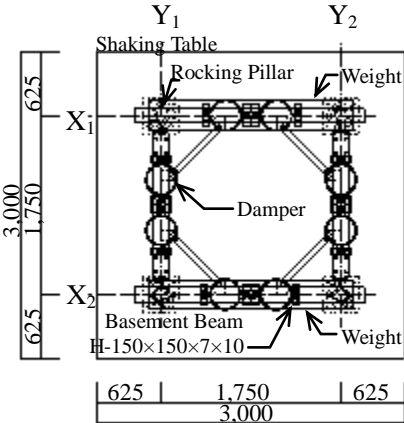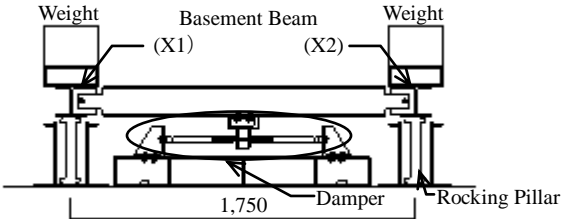
(a) Plan

(c) View of test specimen on shaking table (Case 2)

(b) Section

(d) Rocking pillar

Figure 3. Isolation foundation specimen (unit: mm)

Figure 4. Lead damper installed in test specimen
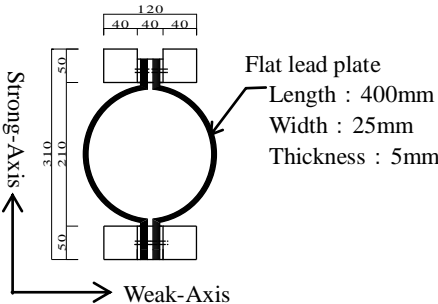
Figure 5. Detail of lead damper (unit: mm)

Table 1. Test cases

Test case	Number of installed steel plate		Mass eccentricity ratio*
	X_1 Beam	X_2 Beam	$X_1 : X_2$
Case1 (Symmetric type)	5	5	1 : 1.00
Case2 (Eccentric type)	3	7	1 : 1.89

* Mass eccentricity ratio indicated in this Table include weight of basement beam

The instrumentation set-up that was used to measure the response of the test specimen to vibration tests is shown in Figure 6. Four accelerometers were fixed on the top of the basement beams (X_1, X_2, Y_1, Y_2) in order to measure response acceleration and a bidirectional accelerometer was attached at center of the shaking table to record input acceleration. Displacement of the basement beams relative to the shaking table was measured using laser displacement sensors and resisting force of the lead damper was measured by a load cell as shown in Figure 6(a).

Translational displacement [mm]

$$X \text{ axis: } \delta_{xt} = \frac{\delta_{x1} + \delta_{x2}}{2}$$

$$Y \text{ axis: } \delta_{yt} = \frac{\delta_{y1} + \delta_{y2}}{2}$$

$$\text{Rotational displacement: } \delta_{xr} = \frac{\delta_{x1} - \delta_{x2}}{2} \text{ [mm]}$$

$$\text{Rotational angle: } \theta = \frac{\delta_{x1} - \delta_{x2}}{\ell} \text{ [rad]}$$

(3.1)

(a) Test setup   (b) Translational and rotational displacement
Figure 6. Instrumentation set-up
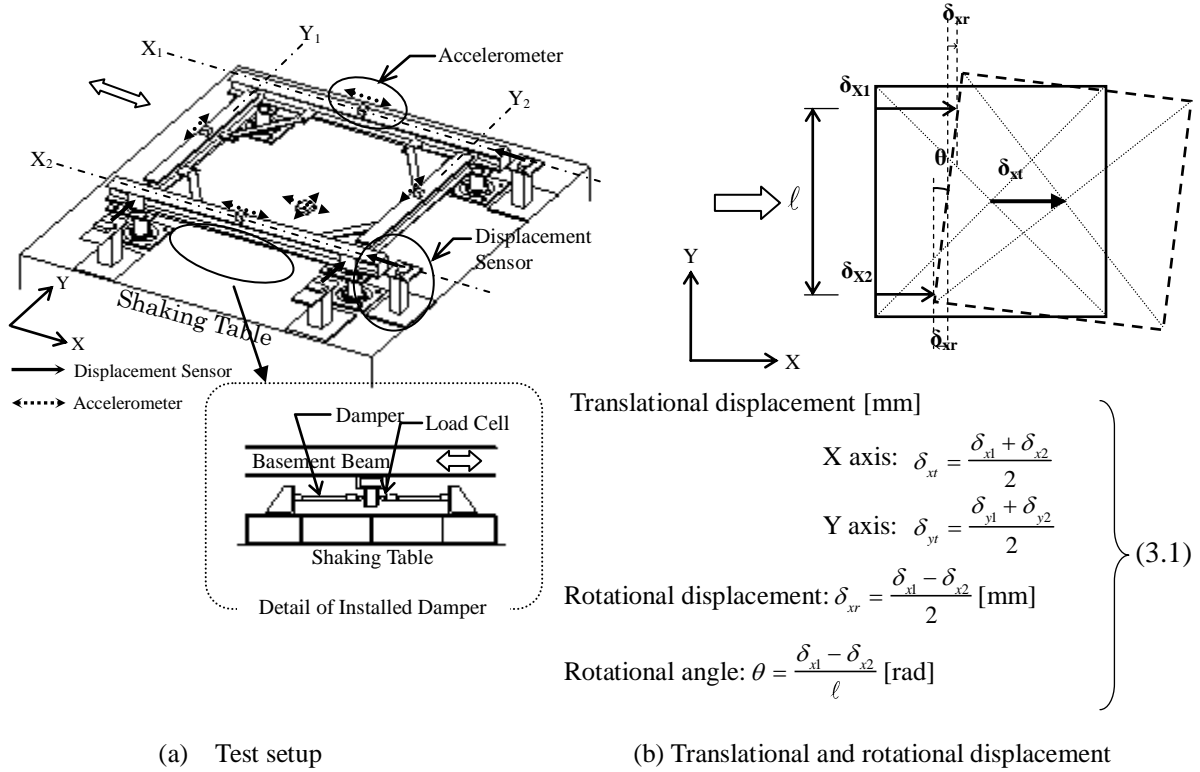
As shown in Figure 6 (b), translational and rotational displacement of the basement beams, δ_{xt}, δ_{yt} and δ_r are calculated by Equation (3.1), where δ_{x1}, δ_{x2}, δ_{y1} and δ_{y2} indicate relative displacement of the basement beams in X_1, X_2, Y_1 and Y_2 axes respectively.

3.2. Shaking Table Test

To verify experimentally the basic characteristics of earthquake response and effect mass eccentricity of superstructure have on seismic performance of the system, the test specimen was subjected to some kind of historical records. The input records are listed in Table 2. The excitation was two-directional. Time axis of the input waves were composed into 1/2 of the original considering that the test specimen was reduced scale model.

Table 2. Input Earthquake Waves

Input Earthquake Wave	Time Axis
El Centro , 1940 Imperial Valley Earthquake	Compressed into 1/2 of original
Tohoku, 1978 Miyagiken-oki Earthquake	
Hachinohe , 1968 Tokachi-oki Earthquake	

As representative test results obtained by excitation of maximum inputs of El Centro wave, time histories for eccentric test case are presented in Figure 7. Furthermore, Table 3 shows comparison of the maximum response parameters of each test case. Figure 8 shows the ratio of translational and torsional displacement to relative displacement of the basement beam at the time of maximum response for each test case.

In symmetric case, response behavior of the basement beam to earthquake input was almost without torsional vibration. Though, an increase in responding displacement due to torsional vibration was observed in the eccentric cases, maximum responding displacement approximately equal that of symmetric case on each test case.

As obtained results, the responding acceleration was largely decreased from the one of shaking table, the range of amplification factors are 0.09-0.56. Maximum responding acceleration of beam on which was put heavier weight showed nearly equal to that of symmetric test case. On the other hand, decrease in the weight of the beam increase responding acceleration of the test specimen. However, even in such case, it has a low responding acceleration amplification factor (0.49).
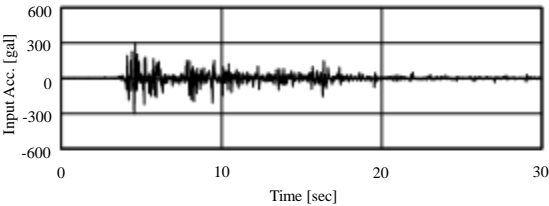
(a) Acceleration of shaking table (X axis) (b) Acceleration of shaking table (Y axis)
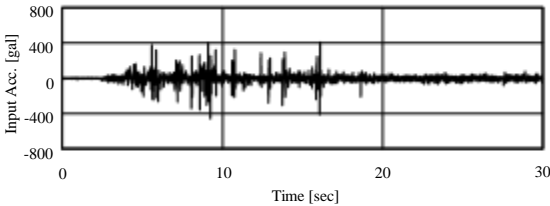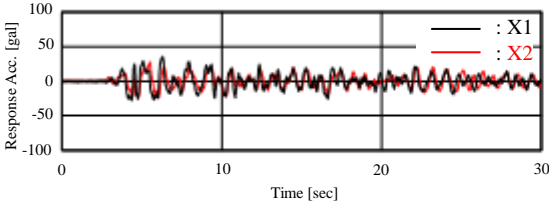
(c) Acceleration of test specimen (X axis) (d) Acceleration of test specimen (Y axis)
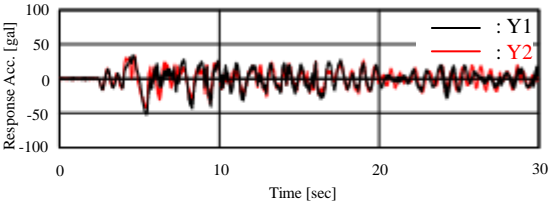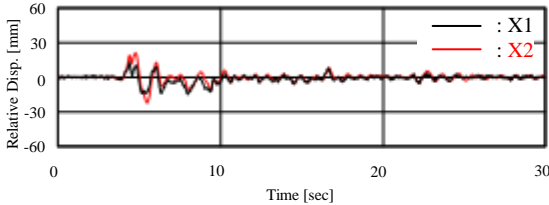
(e) Relative displacement of specimen (X axis) (f) Relative displacement of specimen (Y axis)
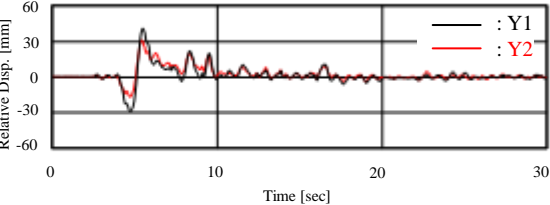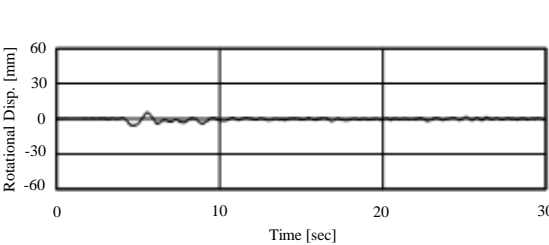
(g) Torsional displacement of specimen (h) Hysteresis Loop of Lead Damper
Figure 7. Response to excitation of El Centro wave, Eccentric weight, Maximum input level
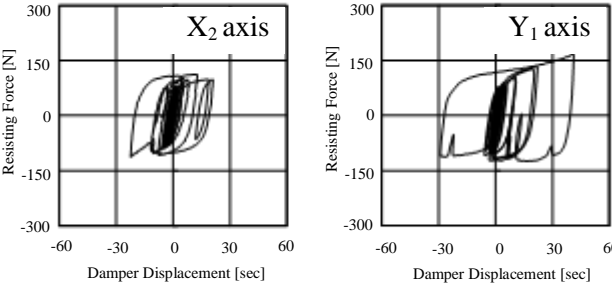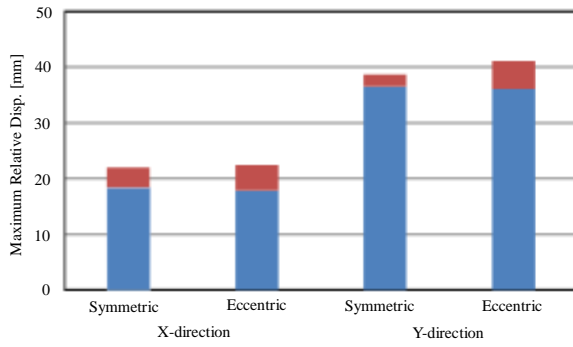
(a) El-Centro Wave
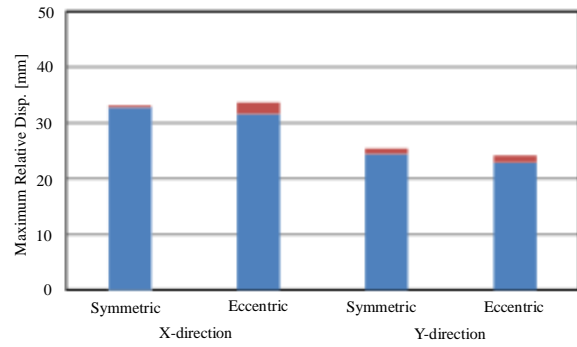
(b) Tohoku Wave
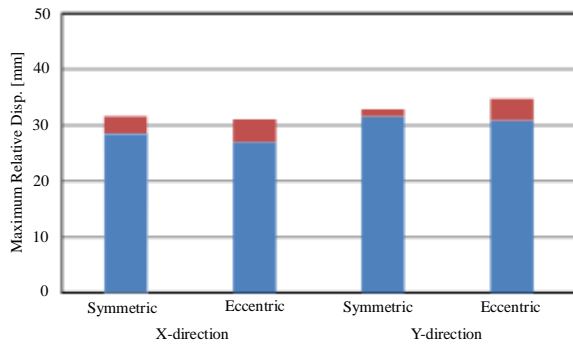
■ : Translatinal Displacement

■ : Torsional Displacement

(c) Hachinohe Wave

Figure 8. Ratio of translational and torsional components included in relative displacement, Maximum level

Table 3. Response to maximum earthquake input

(a) El-Centro Wave

Test Case	Acceleration of Shaking Table [gal]		Maximum Response Acceleration [gal] (Amplification Factor of Acceleration)				Maximum Relative Displacement [mm]				Translation Displacement δ_{xr} [mm]		Maximum Torsional Angle θ [×10⁻³rad]
	X	Y	X1	X2	Y1	Y2	X1	X2	Y1	Y2	X	Y	
Symmetric	156.4	262.6	24.5 (0.16)	22.9 (0.15)	33.9 (0.13)	27.4 (0.10)	10.4	10.3	21.2	17.0	9.5	19.1	3.0
	332.1	490.4	28.9 (0.09)	27.5 (0.08)	47.2 (0.10)	45.0 (0.09)	17.4	22.0	38.7	34.5	18.4	36.5	4.7
Eccentric	148.1	268.9	25.5 (0.17)	21.2 (0.14)	34.7 (0.13)	26.3 (0.10)	9.7	10.6	21.5	15.5	8.6	18.5	4.9
	301.4	460.5	36.2 (0.12)	27.8 (0.09)	51.9 (0.11)	42.3 (0.09)	14.9	22.4	41.1	31.3	17.8	36.1	7.0

(b) Tohoku Wave

Test Case	Acceleration of Shaking Table [gal]		Maximum Response Acceleration [gal] (Amplification Factor of Acceleration)				Maximum Relative Displacement [mm]				Translation Displacement δ_{xr} [mm]		Maximum Torsional Angle θ [×10⁻³rad]
	X	Y	X1	X2	Y1	Y2	X1	X2	Y1	Y2	X	Y	
Symmetric	68.6	60.1	24.1 (0.35)	26.1 (0.38)	19.2 (0.32)	21.2 (0.35)	7.2	7.7	4.7	3.6	7.9	3.7	2.3
	339.8	382.6	40.2 (0.12)	37.6 (0.11)	33.1 (0.09)	34.4 (0.09)	32.8	33.1	25.4	23.6	32.8	24.5	4.0
Eccentric	67.3	59.7	30.2 (0.45)	24.1 (0.36)	19.7 (0.33)	24.8 (0.42)	7.4	8.4	4.6	3.8	7.2	3.7	3.5
	333.0	355.9	44.7 (0.13)	39.2 (0.12)	37.2 (0.10)	37.3 (0.10)	30.2	33.6	24.1	21.8	31.6	22.9	7.9

Table 3. Response to maximum earthquake input
(c) Hachinohe Wave

Test Case	Acceleration of Shaking Table [gal]		Maximum Response Acceleration [gal] (Amplification Factor of Acceleration)				Maximum Relative Displacement [mm]				Translation Displacement δ_{xr} [mm]		Maximum Torsional Angle θ [$\times 10^{-3}$rad]
	X	Y	X1	X2	Y1	Y2	X1	X2	Y1	Y2	X	Y	
Symmetric	40.9	48.3	19.4 (0.47	23.1 (0.56	19.6 (0.41	18.8 (0.39	7.6	9.8	6.0	4.8	8.6	5.4	1.9
	200.3	288.3	30.4 (0.15	35.5 (0.18	35.5 (0.12	40.4 (0.14	27.5	31.6	32.9	31.2	28.5	31.6	4.4
Eccentric	46.3	61.5	22.6 (0.49	20.6 (0.44	24.7 (0.40	22.8 (0.37	6.8	9.6	5.9	4.8	8.2	4.9	3.0
	203.1	259.5	32.5 (0.16	30.4 (0.15	35.9 (0.14	46.9 (0.18	26.8	31.1	27.8	34.7	27.0	30.9	7.3

4. VIBRATION RESPONSE ANALYSIS

4.1. Vibration System and Equation of Motion

To investigate earthquake response characteristics of the rocking pillar base isolation system in two-directional earthquake ground motions, analysis program was developed based on Newmark β method. To verify the validity of the analytical method, the results of shaking table test were compared with those of corresponding numerical simulation by the analysis program. The base isolation system has three degrees of freedom, which are two translational and one rotational components, it can be modeled by vibration system as shown in Figure 9. As for the present lead damper system, the hysteretic resisting force can be idealized by a bilinear model with yield-judgment straight line shown in Figure 10, where parameters are obtained from harmonic excitation test results of the damper.

Figure 9. Vibration system of the test specimen

Figure 10. Analytical model of the damper

Apparent horizontal stiffness of the rocking pillar, $_ik_x$ and $_ik_y$, illustrated in Figure 9, are taken to be

$$K_i = m_i \left(\frac{2\pi}{T}\right)^2 \tag{4.1}$$

where m_i is mass carried on the each rocking pillar and T is natural period of the pillar derived by Equation (2.1). To apply time integration analysis to the model in Figure 9, equation of motion for the vibration system is written as follows for n-th step of discrete time increment.

$$\begin{bmatrix} m & 0 & 0 \\ 0 & m & 0 \\ 0 & 0 & I \end{bmatrix} \begin{Bmatrix} \ddot{x}_{(n)} \\ \ddot{y}_{(n)} \\ \ddot{\theta}_{(n)} \end{Bmatrix} + \begin{bmatrix} K_x & 0 & K_x \cdot e_y \\ 0 & K_y & K_y \cdot e_x \\ K_x \cdot e_y & K_y \cdot e_x & K_\theta \end{bmatrix} \begin{Bmatrix} x_{(n)} \\ y_{(n)} \\ \theta_{(n)} \end{Bmatrix} = -\begin{bmatrix} m & 0 & 0 \\ 0 & m & 0 \\ 0 & 0 & I \end{bmatrix} \begin{Bmatrix} \ddot{x}_{0(n)} \\ \ddot{y}_{0(n)} \\ \ddot{\theta}_{0(n)} \end{Bmatrix} \tag{4.2}$$

where m is a total mass of superstructure, I is a rotation inertia, K_x and K_y are horizontal stiffness of the base isolation foundation in X and Y direction and K_θ is a torsional stiffness. The parameters were determined according to the test data as listed in Table 4. Damping effect of the rocking pillar was

ignored in this analysis for reasons of the test specimen without damper exhibited low damping. As concerns the input ground motion, measured shaking table acceleration was used.

Table 4. Fundamental parameters of the test specimen used in numerical simulation

		Strong Axis : k_{ds}	Weak Axis : k_{dw}
Damper	Initial stiffness : k_1 [N/mm]	38.2	6.69
	Secondary stiffness : k_2 [N/mm]	0.49	0.17
	Initial value : Q_0 [N]	78.4	29.4
	Inclination : β [N/mm]	1.47	0.29
Vibration System	Total Mass : m [ton]	1.30	
	Natural period of the pillar : T [sec]	2.783	
	Overall stiffness of the pillar : $\Sigma_i K_x, \Sigma_i K_y$ [N/mm]	6.63	
	Damping ratio : h [%]	0	
	Rotation inertia : I [$\times 10^5$ Nmm^2]	Case 1 : 147.29 Case 2 : 133.63 Case 3 : 136.44 Case 4 : 112.13 Case 5 : 98.95	
Time step : Δt [sec]		0.005	

4.2. Results of Analysis

Figure 11 shows typical examples of the shaking table test results together with the results of the corresponding numerical simulation. It can be seen that analytical results simulated the test results comparatively well. Similarly, it was confirmed in all cases.

(a) Response acceleration (X_1 Beam)
(b) Response acceleration (X_2 Beam)
(c) Response acceleration (Y_1 Beam)
(d) Response acceleration (Y_2 Beam)
(e) Response displacement (X_1 Beam)
(f) Response displacement (X_2 Beam)
(g) Response displacement (Y_1 Beam)
(h) Response displacement (Y_2 Beam)
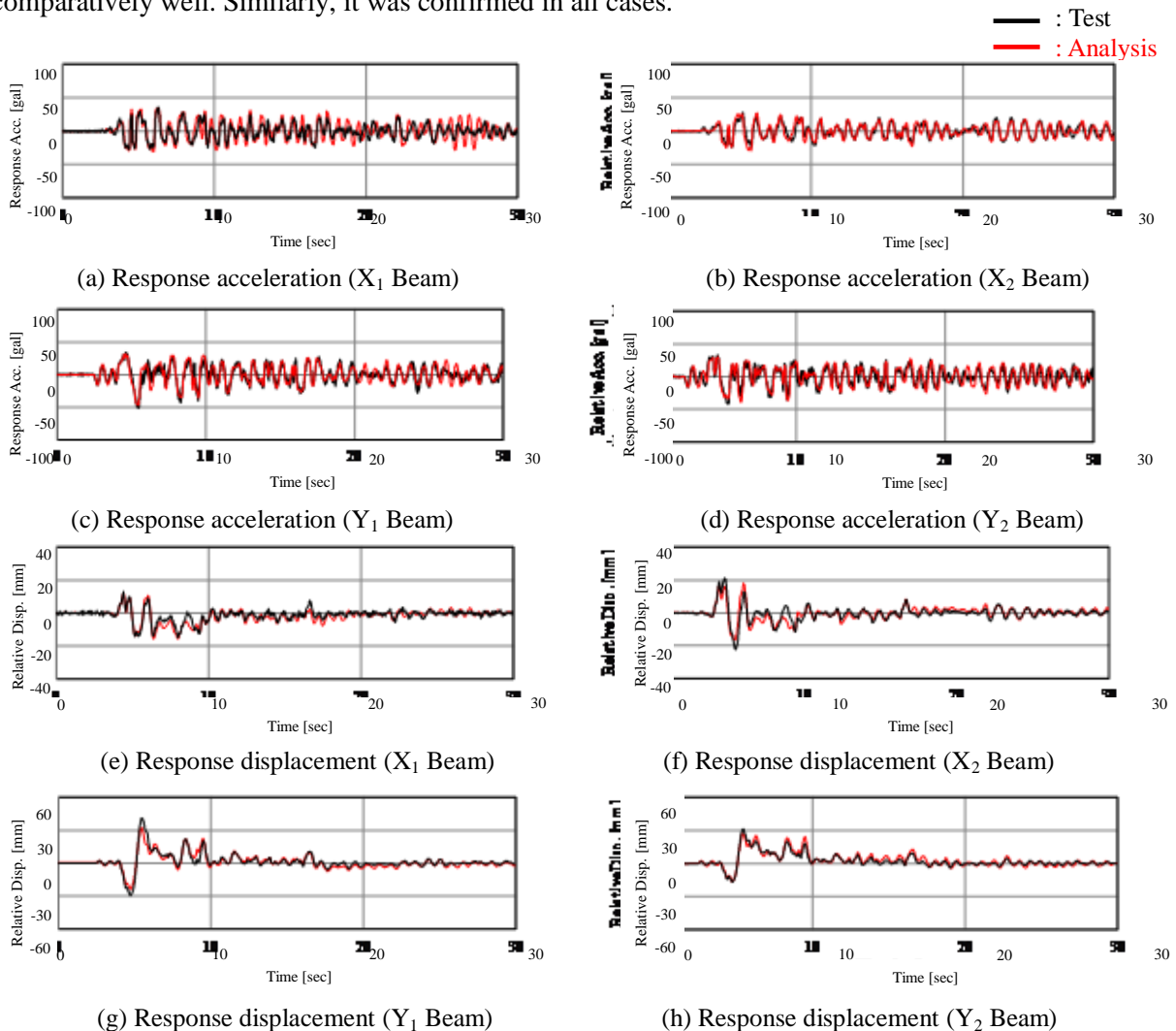
Figure 11. Comparison of response to El Centro wave, Eccentric weight, Maximum input level

5. CONCLUSION

The authors have been developing a new form of base isolation system suitable for masonry houses in developing countries. In the proposed system, a superstructure is supported by rocking pillars which have spherical bearings at the both ends. Two-directional shaking table tests were conducted with regard to a reduced scale test specimen. The fundamental vibration property of the isolation system was made clear based on experiment. Obtained test results indicated promising capability toward the realization of masonry construction with rocking pillar base isolation system. In addition, Numerical analysis by the use of developed program showed fairly good coincidence with the results of the two-directional shaking table tests. As the future direction of this study, we will discuss about effectiveness of full scale model of the isolation system for earthquake wave excitation using developed program.

REFERENCES

EERI/IAEE World Housing Encyclopedia: Earthquake-Resistant Construction of Adobe Buildings: A Tutorial, March 2003.
FUNAKI Naoki, FUJITA Tomomi, HORI Norio, INOUE Norio & KAWAMATA Shigeya: Vibration Response Characteristics of Rocking Pillar Base Isolation System suitable for Masonry Houses, Proceedings of the 14th World Conference on Earthquake Engineering, Paper ID 05-04-0049, Oct. 2008.